

## Formation of GaAs/AlAs(001) interfaces studied by scanning tunneling microscopy

J. Behrend, M. Wassermeier, W. Braun, P. Krispin, and K. H. Ploog

*Paul-Drude-Institut für Festkörperelektronik, Hausvogteiplatz 5-7, D-10117 Berlin, Germany*

(Received 8 September 1995)

We have investigated the interface formation of molecular-beam epitaxy (MBE) grown GaAs/AlAs(001) heterostructures by *in situ* scanning tunneling microscopy (STM) and reflection high-energy electron diffraction (RHEED). Starting from a smooth As-rich ( $2\times 4$ ) reconstructed GaAs surface the formation of the *normal interface* was studied at AlAs layer thicknesses ranging from 1 to 50 ML. With increasing AlAs thickness the reconstruction changes from ( $2\times 4$ ) to ( $2\times 3$ ) via a ( $1\times 1$ ) and a ( $1\times 3$ ) symmetry under the conditions used. For the *inverted interface*, the RHEED pattern changes immediately after the deposition of only 1 ML of GaAs on AlAs from a ( $2\times 3$ ) to a clear ( $2\times 4$ ) symmetry. The STM images of both interfaces show that the interface formation is accompanied by a disordering of the ( $2\times 4$ ) reconstruction by forming kinks in the missing dimer rows that can be related to intrinsic point defects. We attribute the different incorporation of these intrinsic point defects to the different electronic properties of the two interfaces. Large-scale STM images also reveal a different surface roughness for the normal and inverted interface.

### I. INTRODUCTION

Since the precise control of the layer thickness is one of the main advantages of molecular-beam epitaxy (MBE), the study of the interface structure and its influence on device parameters has remained in the mainstream of MBE research since the initial proposal of semiconductor superlattices and quantum wells (QW) by Esaki and Tsu.<sup>1,2</sup> Especially the atomic interface configuration of GaAs/Al<sub>x</sub>Ga<sub>1-x</sub>As heterostructures has played a major role in the progress of advanced device concepts since this material system is commonly used as a model for fundamental studies.<sup>3</sup> Different characterization methods were used to obtain an improved understanding of the complicated interplay between the growth conditions and the actual interface structure.

Using photoluminescence (PL) and photoluminescence excitation (PLE) spectroscopy, a single excitonic peak for a continuously grown GaAs QW and a splitting of this PL/PLE line for a quantum well prepared with growth interruption was found.<sup>4,5</sup> The splitting is attributed to discrete thickness variations of the quantum well on a lateral scale larger than the exciton diameter. A thickness variation smaller than the exciton diameter results in broadened peaks due to the averaging of the exciton wave function over this small size roughness. This behavior is observed for continuously grown samples.

Recent near-field scanning optical microscopy (NSOM) experiments were able to image the morphology of these areas of constant thickness.<sup>6</sup> Depending on the growth conditions, different roughness distributions were detected. Areas from micron size to the resolution limit of NSOM of about 0.1  $\mu\text{m}$  could be imaged.

High-resolution transmission electron microscopy (HRTEM) allows the imaging of semiconductor crystals with atomic resolution,<sup>7,8</sup> but the resulting picture is obtained from a slab typically 50–100 lattice constants thick. Therefore, the unit cell in a HRTEM picture contains information averaged over a column of unit cells along the beam direction, and especially the interpretation of the results concern-

ing the quantitative compositional analysis of interface structures is not clear at the present time.

dc transport was used to study the influence of the interface type on the electron mobility.<sup>9</sup> Si migration during growth towards the inverted interface was found to be the dominant mobility degrading effect.

True atomic resolution can be achieved by probing the cleaved edge of a heterostructure with scanning tunneling microscopy (STM). The results obtained for the GaAs/Al<sub>x</sub>Ga<sub>1-x</sub>As ( $x=0.3$ ) system indicate a demixing of both GaAs and AlAs in the Al<sub>x</sub>Ga<sub>1-x</sub>As regions with a typical modulation length scale of 2 nm.<sup>10,11</sup> This modulation is also present at the interface, causing an interface roughness of the same magnitude.

To understand the known asymmetry in the compositional profile and the electron mobility between the normal interface (AlAs on GaAs) and the inverted interface (GaAs on AlAs) (Refs. 12–14), it is necessary to obtain planar real-space images of the as-grown surfaces. In this paper we report STM results of as-grown AlAs surfaces and of intermediate stages of the formation of the normal and inverted interfaces in the GaAs/AlAs system. Large-scale STM images up to 4000  $\text{\AA}\times 4000 \text{\AA}$  in size reveal the morphological roughness scales of the two interfaces. High-resolution images show that the initial stage of the formation of both interfaces involves disordered reconstructions and a decrease of the overall As coverage due to the incorporation of distinct point defects at the interface planes.

### II. EXPERIMENT

The experiments were carried out in a combined MBE-STM chamber system that allows STM imaging in ultrahigh vacuum (UHV) below  $1\times 10^{-11}$  Torr immediately after MBE growth. Well-oriented epitaxially *n*-type GaAs(001) wafers were used as substrate material. After thermal oxide desorption at 580  $^{\circ}\text{C}$  under an As<sub>4</sub> flux of  $3\times 10^{-6}$  Torr mea-

sured with the ion gauge at the sample position, a 100-nm-thick GaAs layer, Si doped with  $2 \times 10^{18} \text{ cm}^{-3}$ , was grown at a growth rate of 0.5 ML/s and a temperature of 600 °C. These growth conditions were optimized for the preparation of a smooth As-rich ( $2 \times 4$ ) reconstructed surface. The different stages of the formation of the normal interface were realized by deposition of AlAs layers of different thicknesses between 1 and 50 ML with growth rates between 0.1 and 0.3 ML/s. The growth temperature during AlAs deposition was varied over a large range from 540 °C to 630 °C to obtain different reconstructions. To achieve the initial state of the inverted interface configuration 1 ML GaAs was grown on 50 ML AlAs at a temperature of 610 °C and a growth rate of 0.1 ML/s. During growth the sample surfaces were monitored using reflection high-energy electron diffraction (RHEED). To avoid any influence of compensating surface defects due to the Si doping the last 15 ML below the surface of all structures were grown undoped.

After growth we cooled the sample slowly to room temperature and simultaneously lowered the  $\text{As}_4$  background pressure in an optimized way so that the RHEED pattern remained unchanged during the whole process. The resulting surface of this optimized quenching procedure is expected to be similar to the as-grown surface. The transfer of the sample into the STM part of the UHV system was performed at pressures below  $8 \times 10^{-11}$  Torr in a time of about 2 min. The pressure in the STM chamber itself was better than  $1 \times 10^{-11}$  Torr, which allowed tunneling experiments for about 5 h without noticeable oxidation even of pure AlAs. During the STM imaging tip voltages of about 3 V at tunneling currents of 300–700 pA were used. The STM was equipped with electrochemically etched tungsten wire tips that were cleaned *in vacuo* by electron bombardment.

### III. RESULTS AND DISCUSSION

Figure 1(a) shows a typical STM image of the MBE-grown GaAs(001) surface before any AlAs was deposited. A well-ordered ( $2 \times 4$ ) structure with straight As missing dimer rows is observed in accordance with the RHEED pattern shown in Fig. 2 that exhibits well-defined spots on a bright Laue circle in the  $4x$  direction. High-resolution STM images confirm that this reconstruction is composed of two As dimers and two missing dimers per unit cell.<sup>15</sup> Monolayer high  $A$  steps run across the image caused by a slight unintentional miscut of the sample. The large scan STM image of Fig. 1(b) demonstrates the excellent flat morphology of the as-grown GaAs surface before the normal GaAs/AlAs interface is formed. It exhibits atomically flat terraces with a size of several thousand angstroms and small anisotropic islands. This picture reveals the characteristic morphology of the GaAs surface after growth interruption and annealing, which is in our case introduced during the quenching procedure.

In the high-resolution STM image of Fig. 3(a) the surface is seen after deposition of 10 ML of AlAs with a growth rate of 0.1 ML/s at a temperature of 600 °C representing the initial stage of the formation of the normal GaAs/AlAs interface. The ( $2 \times 4$ ) symmetry of the RHEED pattern shown in Fig. 2 remains but becomes streaky, the Laue circle disappears, and the half-order spot of the  $4x$  direction is very weak or vanishes. This finding is correlated to a disordered

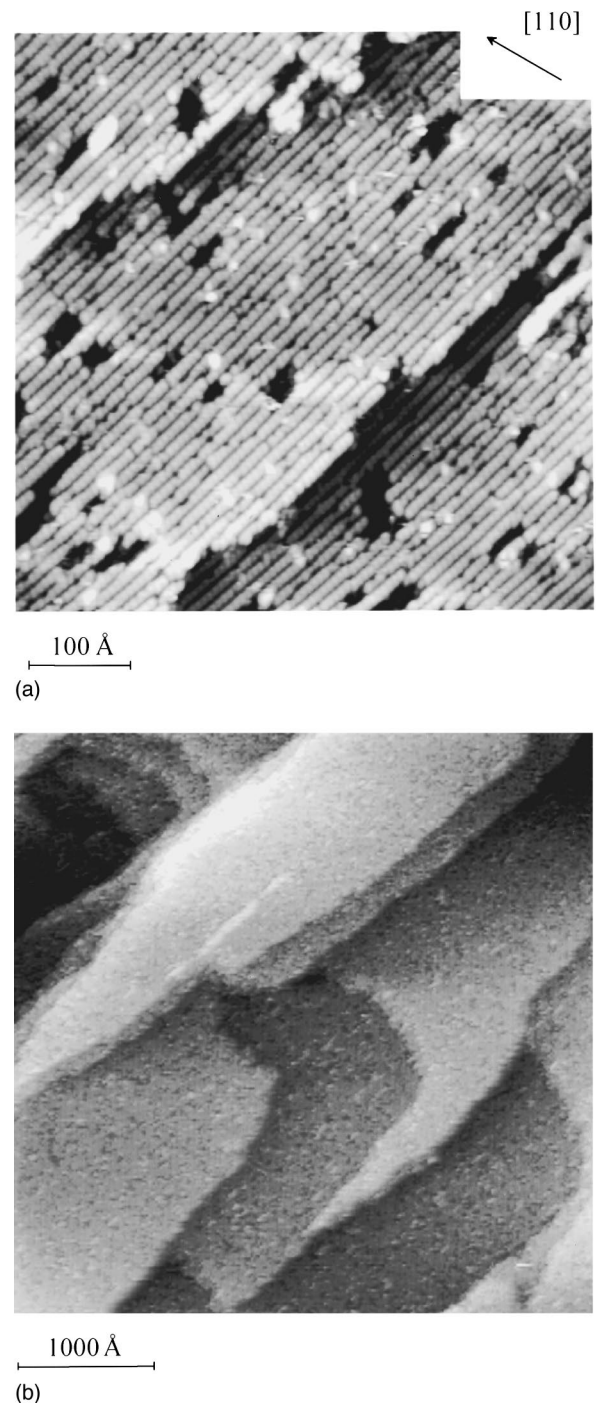


FIG. 1. (a) STM image of the ( $2 \times 4$ ) reconstructed GaAs(001) surface before AlAs deposition, exhibiting a well-ordered ( $2 \times 4$ ) symmetry with straight As missing dimer rows. (b) Large-scan STM image ( $4000 \text{ \AA} \times 4000 \text{ \AA}$ ) of the as-grown GaAs surface being the morphological template for the normal interface.

As missing dimer row structure in the STM data of Fig. 3(a). The STM image reveals a high number of kinks that develop in the missing As dimer rows. A similar behavior of the RHEED pattern as well as of the STM results has been observed also for submonolayer deposition of Si on the GaAs(001) surface.<sup>16,17</sup>

In the case of Si deposition, the kink formation is attributed to the creation of compensating surface defects due to

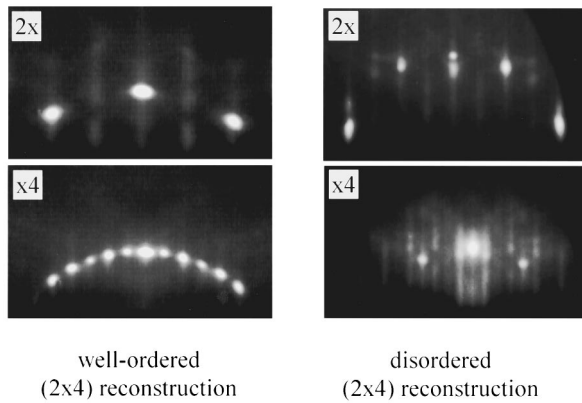


FIG. 2. RHEED pattern of a well-ordered and a disordered (2 $\times$ 4) reconstruction before and after AlAs was deposited. The characteristic weakening of the half-order spot in the 4x direction is observed indicating the kink creation.

the added  $n$ -type dopants to keep the Fermi level at midgap.<sup>18</sup> At first glance, this explanation does not seem to be reasonable for the incorporation of isoelectronic species like Al in GaAs. But, from recent deep-level transient spectroscopy (DLTS) measurements, it is known that during AlAs

growth intrinsic point defects identified as As vacancies are created at the surface.<sup>19</sup> The As vacancy in bulk GaAs produces a series of defect levels of  $t_2$  symmetry in the upper part of the band gap.<sup>20</sup> In Ref. 19 it was shown that also in the AlAs material defect levels are created close to the conduction band due to negatively charged As vacancies. From scanning tunneling spectroscopy investigations on GaAs(001) the position of the Fermi level at the surface could be derived. For undoped material or at lower doping levels ( $< 1 \times 10^{18} \text{ cm}^{-3}$ ) the intrinsic surface defects such as steps and imperfections of the reconstruction provide enough surface states to pin the Fermi level at a midgap position without kink formation.<sup>18</sup> Therefore, during the creation of the As vacancy at the AlAs/GaAs growth front electrons can be released because the corresponding defect level is always located above the pinned Fermi energy and the compensating kinks appear. AlAs deposition on the GaAs(001) surface will produce compensating surface defects in response to electronic states, which originate from As vacancies inherent to the AlAs surface during growth.

The observed slow transient in the disorder at the normal interface is related to the strong segregation of Ga in AlAs that was deduced from phase shift measurements of the RHEED intensity oscillations during the initial stage of the

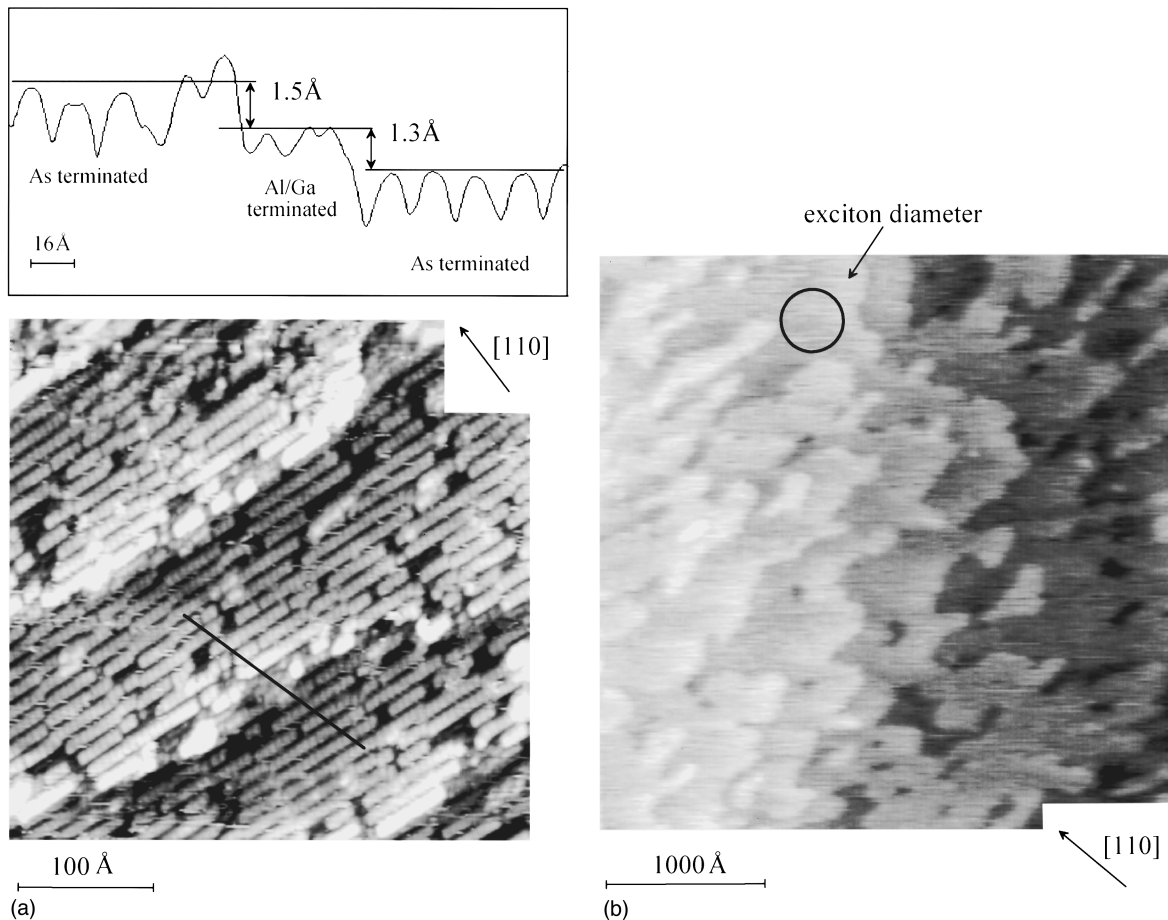


FIG. 3. (a) STM image of the surface after 10 ML AlAs deposition, revealing an increasing amount of disorder due to kinking and a decrease of the As coverage. The cross-sectional profile taken across the exposed region at the step edge shows the stacking sequence of the atomic planes made of As and Al and/or Ga. (b) Large-scale STM image (3500 Å $\times$ 3500 Å) of a 50-ML-thick AlAs(001) layer revealing the as-grown surface morphology. The shape, size, and distribution of the islands and terraces are found to be similar to the GaAs(001) surface with only a slightly elevated degree of roughness. The solid circle indicates the generally used average exciton diameter for comparison.

interface formation.<sup>21,22</sup> As a consequence, the STM images after AIAs deposition between 1 and 10 ML show the structure of an  $\text{Al}_x\text{Ga}_{1-x}\text{As}$  surface alloy with a large  $x$  value instead of an intrinsically reconstructed AIAs layer. In addition, Ga segregation and intermixing effect are expected to be enhanced in the present case due to the long duration of the quenching procedure.

The initial stage of the formation of the normal GaAs/AIAs interface is additionally accompanied by a decrease of the As coverage. Primarily at the step edges, the Al and/or Ga layer is exposed and shows a disordered structure of short chains along the step direction. The terraces as well exhibit holes that expose the atomic plane below [see Fig. 3(a)]. A cross-sectional profile taken perpendicular to the step direction [shown in the upper part of Fig. 3(a)] reveals that the height of the feature at the step edge is approximately halfway between the adjacent two As-terminated terraces. Therefore, it can be assigned to the atomic plane consisting of Al and/or Ga. A chemical contrast between the Al and Ga atoms similar to the results of cross-sectional STM on the (110) cleaved edge could not be detected.

Figure 3(b) shows a large scan STM image of a 50-ML-thick AIAs layer deposited with a growth rate of 0.3 ML/s at a temperature of 610 °C. During growth the RHEED pattern changes from a well-defined  $(2 \times 4)$  to a very weak  $(2 \times 3)$  reconstruction via a  $(1 \times 1)$  and a  $(1 \times 3)$  symmetry, indicating that only a weakly ordered reconstruction is formed on this surface. The indistinct RHEED pattern leads us to conclude that the intrinsic point defects are always present at the AIAs surface during growth without being incorporated into the layer. The thick layer grown this way is expected to exhibit more intrinsic properties of the AIAs material, because Ga segregation has terminated.<sup>21,22</sup> Further, the image in Fig. 3(b) can provide information about the interface configuration as it represents the stage prior to the formation of the inverted interface. The picture in Fig. 3(b) shows the AIAs surface to be surprisingly smooth with monolayer high steps and islands arranged similar to the GaAs(001) surface grown without annealing.<sup>23</sup> The imaged AIAs surface represents a steady-state structure during two-dimensional nucleated growth with a typical length scale of about 30 nm and a large degree of anisotropy. In particular the step edges are rough and show pronounced meandering. We find a RMS (root mean square) surface height fluctuation on this surface of about 2.28 Å. This value is comparable to the RMS roughness of the GaAs(001) surface grown without annealing.

In a next step we have produced the initial stage of the inverted AIAs/GaAs interface by the deposition of 1 ML GaAs on a 50-ML-thick AIAs layer using a growth rate of 0.1 ML/s at a temperature of 580 °C. During growth, the RHEED pattern changes very rapidly from the  $(2 \times 3)$  to a clear  $(2 \times 4)$  symmetry with the characteristic weak half-order spot. The pattern looks very similar to the one that was present after AIAs deposition during the formation of the normal GaAs/AIAs interface (see Fig. 2), indicating a disordered  $(2 \times 4)$  reconstruction. The high-resolution STM image in Fig. 4(a) confirms this expectation. A high degree of disorder introduced by kink formation and a decreased As coverage are visible. In contrast to the normal interface, the kink density is remarkably higher, indicating a high intrinsic point defect density at the growing AIAs sur-

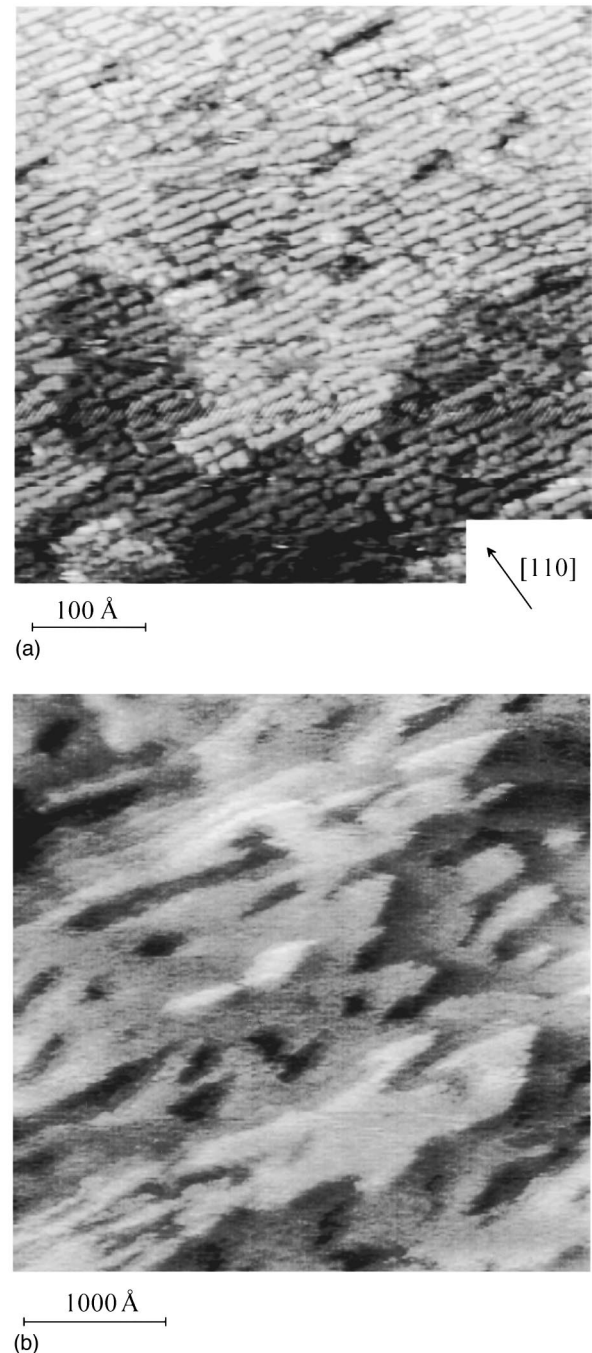


FIG. 4. (a) High-resolution STM image of the inverted interface after growth of 1 ML GaAs on AIAs. A large number of kinks and the decrease of the As coverage are visible. (b) Large-scale STM image ( $4000 \text{ \AA} \times 4000 \text{ \AA}$ ) of the inverted interface after 1 ML of GaAs was deposited. It reveals a relatively smooth morphology comparable to the AIAs surface shown in Fig. 3(b).

face. At the inverted AIAs/GaAs interface these defects are buried at the interface plane due to the abrupt phase transition of the reconstruction from  $(2 \times 3)$  to  $(2 \times 4)$  and the absence of segregation or intermixing. The large scan STM image of the surface shown in Fig. 4(b) confirms the impression of Fig. 3(b) that the inverted interface also exhibits a relatively smooth morphology not drastically different from the normal interface.

Together with our findings of reduced As coverage and

the kink formation during the initial stage of the configuration of both interface types, the relatively smooth morphology at the inverted interface leads us to conclude that morphological roughness alone cannot explain the large asymmetry in electronic properties between normal and inverted interfaces. Instead, the creation of intrinsic point defects at the interface planes plays an important role. Starting from the GaAs surface without kinks, the normal GaAs/AlAs interface is formed with a continuous reconstruction change extending about 10 ML into the AlAs. This directly confirms the strong Ga segregation in AlAs with kink formation corresponding to the Al content and a reduced As coverage during this intermediate stage. The starting kink formation is related to the occurrence of intrinsic defect levels during AlAs growth. These point defects were identified as negatively charged As vacancies in the bulk.<sup>19</sup> Therefore, they can release electrons due to their energetic position above the midgap pinned Fermi level at the surface and act as virtual donors. A very diffuse RHEED pattern is observed for AlAs growth, indicating a disordered reconstruction. We speculate that during this time the growth front features electronic defects that remain close to the surface without being incorporated into the layer. In contrast to the normal interface the formation of the inverted AlAs/GaAs interface takes place very rapidly. Already after the deposition of the first ML of GaAs the phase transition of the reconstruction is complete and the surface appears more ordered again. This is the reason why a high intrinsic defect density is incorporated at the inverted AlAs/GaAs interface leading to a large number of kinks in the STM images.

In this sense, the occurrence of surface compensating defects resulting in the formation of kinks of the  $(2 \times 4)$  reconstruction allows us to image the growth inherent generation of intrinsic defects (As vacancies) during the AlAs growth at both interface planes. The Ga segregation at the normal interface and the abruptness of the phase transition at the inverted interface cause the asymmetry between both interface types. This assumption is in excellent agreement with recent DLTS measurements, which have shown that specific deep-level defects attributed mainly to As vacancies are present at the inverted interface.<sup>19</sup>

#### IV. SUMMARY

We have imaged the formation of MBE-grown GaAs/AlAs(001) interfaces and the as-grown AlAs surface by *in situ* STM. Images of the initial stage of the formation of both interface types reveal a high degree of disorder of the reconstruction due to kink formation and a decrease of the overall As coverage. Our result sheds new light on the question of kink formation on the  $(2 \times 4)$  reconstructed GaAs surface. The presence of kinks after the deposition of isoelectronic species reveals the creation of compensating surface defects in response to intrinsic deep-level defects at the growth front. We attribute the occurrence of kinks during the initial stages of AlAs/GaAs interface formation to the growth-inherent creation of As vacancies at the AlAs surface. Due to the position of the corresponding defect states above the midgap pinned Fermi level at the surface, these intrinsic point defects act as donors and compensating kinks appear. The asymmetry between both interface types is caused by the incorporation of the defect layer at the growing AlAs surface during the abrupt formation of the inverted interface. This finding is supported by the surprisingly high quality of the morphology of the as-grown AlAs(001) surface that is evident from our large-scale STM images. We find a degree of roughness that is only slightly larger compared with the GaAs(001) surface and a similar step and island arrangement. As STM scans from the stage directly after the interface formation show, this morphology is preserved at the inverted interface too. Using these results at the inverted interface, we can conclude that, additionally to the previously reported Si migration effect, the incorporation of intrinsic point defects plays an important part in reducing the electron mobility in two-dimensional electron gas heterojunctions.

#### ACKNOWLEDGMENTS

The authors would like to thank H. P. Schönherr for his expert help with the experimental setup and valuable discussions and K. J. Friedland for critical reading of the manuscript. Part of this work was sponsored by the Bundesministerium für Bildung, Wissenschaft, Forschung und Technologie and the Deutsche Forschungsgemeinschaft (SFB 296).

- 
- <sup>1</sup>L. Esaki and R. Tsu, IBM J. Res. Dev. **14**, 61 (1970).  
<sup>2</sup>L. Esaki and R. Tsu, Appl. Phys. Lett. **22**, 562 (1973).  
<sup>3</sup>C. Weidbüsch, J. Cryst. Growth **127**, 742 (1993).  
<sup>4</sup>B. Orschel, G. Oelgart, R. Houdré, M. Proctor, and F. K. Reinhardt, Appl. Phys. Lett. **62**, 843 (1993).  
<sup>5</sup>T. Schweizer, K. Köhler, P. Ganser, D. J. As, and K. H. Bachem, Superlatt. Microstruct. **8**, 179 (1990).  
<sup>6</sup>H. F. Hess, E. Betzig, T. D. Harris, L. N. Pfeiffer, and K. W. West, Science **264**, 1740 (1994).  
<sup>7</sup>N. Ikarashi, T. Baba, and K. Ishida, Appl. Phys. Lett. **62**, 1632 (1993).  
<sup>8</sup>A. Poudoulec, B. Guenais, C. D. Anterrosches, P. Auvray, M. Baudet, and A. Regreny, Appl. Phys. Lett. **60**, 2406 (1992).  
<sup>9</sup>L. Pfeiffer, E. F. Schubert, K. W. West, and C. W. Magee, Appl. Phys. Lett. **58**, 2258 (1991).  
<sup>10</sup>M. B. Johnson, U. Maier, H. P. Meier, and H. W. M. Salemink, Appl. Phys. Lett. **63**, 1273 (1993).  
<sup>11</sup>O. Albrektsen, H. P. Meier, D. J. Arent, and H. W. M. Salemink, Appl. Phys. Lett. **62**, 2105 (1993).  
<sup>12</sup>T. Sajoto, M. Santos, J. J. Heremans, and M. Shayegan, Appl. Phys. Lett. **54**, 840 (1989).  
<sup>13</sup>L. Pfeiffer, K. W. West, H. L. Störmer, and K. W. Baldwin, Appl. Phys. Lett. **55**, 1888 (1989).  
<sup>14</sup>T. Saku, Y. Hirayama, and Y. Horikoshi, Jpn. J. Appl. Phys. **30**, 902 (1991).  
<sup>15</sup>T. Hashizume, Q. K. Xue, J. Zhou, A. Ichimiya, and T. Sakurai, Phys. Rev. Lett. **73**, 2208 (1994).  
<sup>16</sup>M. D. Pashley and K. W. Haberern, Phys. Rev. Lett. **67**, 2697 (1993).  
<sup>17</sup>M. Wassermeier, J. Behrend, L. Däweritz, and K. H. Ploog, Phys. Rev. B **52**, R2269 (1995).

- <sup>18</sup>M. D. Pashley, K. W. Habermann, R. M. Feenstra, and P. D. Kirchner, *Phys. Rev. B* **48**, 4612 (1993).
- <sup>19</sup>P. Krispin, R. Hey, and H. Kostial, *J. Appl. Phys.* **77**, 5773 (1995).
- <sup>20</sup>H. Xu and U. Lindefelt, *Phys. Rev. B* **41**, 5979 (1990).
- <sup>21</sup>W. Braun and K. H. Ploog, *J. Appl. Phys.* **75**, 1993 (1994).
- <sup>22</sup>W. Braun and K. H. Ploog, *Appl. Phys. A* **60**, 441 (1995).
- <sup>23</sup>J. Sudijono, M. D. Johnson, M. B. Elowitz, C. W. Snyder, and B. G. Orr, *Surf. Sci.* **280**, 247 (1993).